STRUCTURAL STUDY OF LANGMUIR MONOLAYERS CONTAINING LIPIDATED POLY(ETHYLENE GLYCOL) AND PEPTIDES

by

Havazelet Bianco-Peled
Department of Chemical Engineering
Technion-IIT Haifa, Israel 32000
and
Yoav Dori and James Schneider
Department of Chemical Engineering and Materials Science
University of Minnesota, Minneapolis
Minnesota 55455 USA
and
Li-Piin Sung and Sushil Satija
National Institute of Standards and Technology
Gaithersburg, MD 20899 USA
and
Matthew Tirrell
Department of Chemical Engineering and Materials Science
Materials Research Laboratory
University of California Santa Barbara
Santa Barbara, California 93106 USA

Reprinted from Langmuir, Vol. 17, No. 22, 6931-6937, 2001.

NOTE: **This paper is a contribution of the National Institute of Standards and Technology and is not subject to copyright.**

NIST CENTENNIAL 1901-2001

NIST
National Institute of Standards and Technology
Technology Administration, U.S. Department of Commerce

Structural Study of Langmuir Monolayers Containing Lipidated Poly(ethylene glycol) and Peptides

Havazelet Bianco-Peled,[†] Yoav Dori,[‡] James Schneider,[‡,§] Li-Piin Sung,[||] Sushil Satija,[||] and Matthew Tirrell*,[⊥]

Department of Chemical Engineering, Technion−IIT Haifa, Israel 32000, Department of Chemical Engineering and Materials Science, University of Minnesota, Minneapolis, Minnesota 55455, Center for Neutron Research, National Institute of Standards and Technology, Gaithersburg, Maryland 20899, and Departments of Chemical Engineering and Materials, Materials Research Laboratory, University of California Santa Barbara, Santa Barbara, California 93106

Received April 2, 1999. In Final Form: August 15, 2001

The structure of Langmuir monolayers containing either a lipidated poly(ethylene glycol) (PEG-lipid) or a lipidated peptide (peptide-amphiphile) or a binary mixture of both was studied using neutron reflectivity. The PEG portion of the PEG-lipid extends into the water, forming dense polymer "brushes". The PEG volume fraction profiles and the brush height were evaluated from the reflectivity curves for monolayers containing PEG-lipids with PEG molecular masses of 120, 750, 2000, and 5000 Da at various grafting densities. At relatively low surface densities, the segmental concentration profile for DSPE-PEG5000 (1,2-distearoyl-*sn*-glycero-3-phosphoethanolamine-*N*-[(ethylene glycol)$_n$], DSPE) and DSPE-PEG2000 was well-described by the parabolic profile predicted by the analytical self-consistent mean field theory. An increase in the surface density produced "flattening" of the profile, which became more pronounced as the chain length decreased. The dependence of the brush height on the surface density and the chain length was in close agreement with the power laws predicted by the self-consistent mean field and the scaling theories. Unlike the flexible PEG chains, the peptide-amphiphile that was used in this study has a stiff conformation. The headgroup is oriented perpendicular to the air−water interface, and this configuration is nearly unaffected by changes in the surface density. Incorporation of the peptide-amphiphile into a PEG-lipid monolayer results in perturbation of the brush structure, due to the enhanced configuration constraints. These studies enable us to gauge how the tethered peptide in the monolayer can be exposed or masked when mixed with tethered PEG chains.

Introduction

The properties of tethered polymer chains have been studied extensively from both a theoretical and an experimental perspective.[1] In addition to fundamental scientific interest, polymer brushes have been proposed for a wide range of practical applications, such as stabilization of colloidal dispersions, adhesion, and lubrication.[2−4] In recent years, there is an increasing interest in the potential applications of water-soluble polymers in biological systems, in particular surface modifications of biomaterials and particulate microcarrier systems used in drug delivery.[5,6] One of the most suitable polymers for these applications is poly(ethylene glycol) (PEG), due to its low protein adsorption, chemical inertness, biocompatibility, and nonionic character, which makes it insensitive to solution ionic conditions.[6] Grafted PEG chains have been used to make sterically stabilized liposomes, and it has been shown that the incorporation of lipids, with a PEG headgroup (PEG-lipids), can enhance dramatically the in vivo circulation time of these liposomes.[5,7,8]

Most of the studies of the physical properties of tethered PEG layers, which generally consist of very short chains, have concluded that the results can be described by theories that were developed for high molecular weight polymers. For example, the average thickness of a PEG layer in the "mushroom" regime is comparable to the Flory radius of the polymer and increases (in the "brush" regime) as the area per molecule decreases.[9−13] This trend of thickness changes agrees, at least quantitatively, with the Alexander−de Gennes model[14,15] for high molecular weight polymers. Sarmoria and Blankschtein[16] have utilized the rotational isomeric state model, which neglects

* To whom correspondence should be addressed.
[†] Technion−IIT Haifa.
[‡] University of Minnesota.
[§] Current address: Department of Chemical Engineering, Carnegie Mellon University, Pittsburgh, PA 15213.
[||] National Institute of Standards and Technology.
[⊥] University of California Santa Barbara.

(1) Halperin, A.; Tirrell, M.; Lodge, T. P. *Adv. Polym. Sci.* **1991**, *100*, 31.
(2) Napper, D. H. *Polymeric Stabilization of Colloidal Dispersions*; Academic Press: New York, 1983.
(3) Piirma, I. *Polymeric Surfactants*; Surface Science Series 42; Marcel Dekker: New York, 1992.
(4) Wu, S. *Polymer Interfaces and Stability*; Marcel Dekker: New York, 1982.
(5) Woodle, M. C.; Lasic, D. D. *Biochim. Biophys. Acta* **1992**, *1113*, 171.
(6) Kuhl, T. L.; Leckband, D. E.; Lasic, D. D.; Israelachvili, J. N. *Biophys. J.* **1994**, *66*, 1479.
(7) Allen, T. A.; Hansen, C.; Martin, F.; Redemann, C.; Yau-Young, A. *Biochim. Biophys. Acta* **1991**, *1066*, 29.
(8) Blume, G.; Ceve, G. *Biochim. Biophys. Acta* **1990**, *1029*, 91.
(9) Janzen, J.; Song, X.; Brooks, D. E. *Biophys. J.* **1996**, *70*, 313.
(10) Kenworthy, A. K.; Hristova, K.; Needham, D.; McIntosh, T. J. *Biophys. J.* **1995**, *68*, 1921.
(11) Majewski, J.; Kuhl, T. L.; Gerstenberg, M. C.; Israelachvili, J. N.; Smith, G. S. *J. Phys. Chem. B* **1997**, *101*, 3122.
(12) Majewski, J.; Kuhl, T. L.; Kjaer, K.; Gerstenberg, M. C.; Als-Nielsen, J.; Israelachvili, J. N.; Smith, G. S. *J. Am. Chem. Soc.* **1998**, *120*, 1469.
(13) Kuhl, T. L.; Majewski, J.; Wong, J. Y.; Steinberg, S.; Leckband, D. E.; Israelachvili, J. N.; Smith, G. S. *Biophys. J.* **1998**, *75*, 2352.
(14) Alexander, S. *J. Phys.* (*Paris*) **1977**, *38*, 983.
(15) de Gennes, P. G. *Macromolecules* **1981**, *14*, 1637.
(16) Sarmoria, C.; Blankschtein, D. *J. Phys. Chem.* **1992**, *96*, 1978.

10.1021/la990383i CCC: $20.00 © 2001 American Chemical Society
Published on Web 09/29/2001

long-range excluded volume effects, for the calculation of the root mean square end-to-end distance of isolated PEG chains. They showed that the calculated dimensions of terminally grafted chains, which are longer than 10 units, are in good agreement with the predictions of the polymer scaling laws[17,18] for chains under θ-solvent conditions. Kuhl et al.[6] have modeled force profiles between two PEG-containing bilayers using the Dolan and Edwards[19] theory for the "dilute mushroom" regime and the Alexander–de Genes model[14,15] for the brush regime and concluded that these theories could be applied to systems of short chains. Kenworthy et al.[10] compared experimental pressure–distance relations with the predictions of modified forms of the Hristova and Needham,[20] de Gennes,[21] and Milner et al.[22] theories. Although none of these theories was sufficient to account for the entire range of measured data, a reasonable fit to one of them could be obtained in a given pressure regime, chain length, and surface density. Neutron and X-ray reflectivity data[11−13] were best fitted when the density distribution of the PEG segments was assumed to be parabolic, as predicted by the analytical self-consistent mean field theory.[22] On the other hand, Szleifer[23,24] argued that the analytical self-consistent mean field and the scaling theories are not valid for systems of short chains. His theoretical single-chain, mean field calculations have shown that the brush thickness agrees with the predictions of the analytical theories, probably due to lack of sensitivity to the assumption of infinitely long chains. However, these predictions do not hold to other thermodynamic properties, such as osmotic pressure in the layer. Moreover, an "extended mushroom" conformation was observed even at very low grafting densities, with a broad mushroom-to-brush transition. Recently, Rex et al.[25] combined affinity of binding measurements and Monte Carlo simulations to study the structure of PEG layers. They have concluded that the chains are in the mushroom regime even when the distances between the grafting points are well below the Flory radius, a finding that seems to support the existence of a broad mushroom-to-brush transition.

Most of the previous work on PEG-lipid systems has focused on monolayers containing a relatively low concentration (typically 1−10 mol %) of PEG-lipid mixed with lipids bearing nonpolymer headgroups, a concentration range that is considered to be optimal for the stabilization of liposomes. There are, however, applications for which a higher surface density of the polymer is preferred. An example of such an application is membranes with controlled biological activity, which are described in a companion paper.[26] The active component in these membranes is a peptide-amphiphile, a synthetic molecule in which a peptide headgroup is covalently linked to lipid tails.[27] The peptide-amphiphile that we used is designated $(C_{16})_2$-Glu-C_2-$(GPP^*)_4$-IVH1.[28] The peptide headgroup contains a 15 amino acid sequence from the triple-helical domain of type IV collagen, known as peptide IVH1. This peptide is known to play an important role in murine melanoma cell adhesion, motility, invasion of basement membranes, and metastasis.[29] The $(GPP^*)_4$ repeat and dialkyl tails induce the IVH1 peptide to fold into a stable triple-helical conformation.[28] In contrast to the peptide-amphiphile, PEG-lipids are effective in preventing protein and cell adhesion to surfaces.[30,31] We have shown that the headgroup length of a PEG-lipid, incorporated into a membrane containing a peptide-amphiphile, determines the accessibility of the peptide ligand to cell surface receptors and thus the interaction of the membrane with cells. When the PEG chains are much shorter than the peptide, the peptide ligand is fully exposed and can be recognized by the cell receptors. On the other hand, PEG chains that are much longer than the peptide mask the ligand completely, resulting in a membrane surface that is inert to cells.

In this paper, we present the results of a detailed neutron reflectivity study, aimed at understanding the behavior of membranes containing a PEG-lipid, a peptide-amphiphile, or a binary mixture of both. In the first part, we focus on PEG-lipid monolayers at the air–water interface in the limit of very high surface densities. The structure of the PEG brushes is compared with theoretical predictions and with previous work on dense brushes.[31] The second part examines the conformation of the peptide-amphiphile headgroup and its dependence on the grafting density. Finally, we consider mixed membranes and show that incorporating a peptide-amphiphile into a PEG-lipid monolayer perturbs the brush structure and can be used to manipulate sterically the accessibility of the peptide.

Experimental Section

Materials. The synthesis of the peptide-amphiphile is described elsewhere.[27] PEG-lipids, 1,2-distearoyl-*sn*-glycero-3-phosphoethanolamine-*N*-[(ethylene glycol)$_n$] (DSPE), with n = 3, 17, 45, and 113 (DSPE-PEG120, DSPE-PEG750, DSPE-PEG2000, and DSPE-PEG5000), were obtained from Avanti Polar Lipids, Inc. Chloroform and methanol (Aldrich) were of HPLC grade. Water was deionized and purified in a Milli-Q (Millipore) system to a final resistivity of 18.2 MΩ cm. Deuterium oxide (99% D) was obtained from Cambridge Isotope Laboratories, Inc.

Procedures. Neutron reflectivity measurements were carried out on the NG-7 reflectometer at the National Institute of Standards and Technology (NIST), Gaithersburg, MD. An in situ Teflon Langmuir trough, equipped with a vibration reduction system, was used. The amphiphiles were spread on the air–water interface from solutions of about 1 mg/mL in a 99:1 chloroform/methanol mixture, using a Hamilton microsyringe. Surface pressure (π) was monitored using a filter paper Wilhelmy plate and a Nima microbalance. The intensity of the speculary reflected beam (R_b) was measured as a function of the wave vector $q = 4\pi/\lambda \sin\theta$, where θ is the angle of incidence and λ = 4.8 Å is the wavelength of the neutron beam. The wavelength spread ($\Delta\lambda/\lambda$) was about 2.5%. The background intensity was estimated from the intensity reflected at angles close to the specular angle and subtracted from R_b. The corrected reflectivity (R) is given as the ratio of reflected to incident intensity.

(17) Flory, P. J. *Principles of Polymer Chemistry*; Cornell University Press: New York, 1953.
(18) de Gennes, P. G. *Scaling Concepts in Polymer Physics*; Cornell University Press: New York, 1979.
(19) Dolan, A.; Edwards, F. *Proc. R. Soc. London, Ser. A* **1974**, *337*, 509.
(20) Hristova, K.; Needham, D. *J. Colloid Interface Sci.* **1994**, *168*, 302.
(21) de Gennes, P. G. *Adv. Colloid Interface Sci.* **1987**, *27*, 189.
(22) Milner, S.; Witten, T.; Cates, M. *Macromolecules* **1988**, *21*, 2610.
(23) Szleifer, I. *Curr. Opin. Colloid Interface Sci.* **1996**, *1*, 416.
(24) Szleifer, I.; Carignano, M. A. In *Advances in Chemical Physics*; Prigogine, I., Rice, S. A. I., Eds.; John Wiley and Sons: New York, 1996; Vol. XCIV, p 165.
(25) Rex, S.; Zuckermann, M. J.; Lafleur, M.; Silvius, J. R. *Biophys. J.* **1998**, *75*, 2900.
(26) Dori, Y.; Bianco-Peled, H.; McCarthy, J. B.; Tirrell, M. *J. Biomed. Mater. Res.* **2000**, *50*, 75.
(27) Berndt, P.; Fields, G.; Tirrell, M. *J. Am. Chem. Soc.* **1995**, *117*, 9515.
(28) Yu, Y. C.; Berndt, P.; Tirrell, M.; Fields, G. *J. Am. Chem. Soc.* **1996**, *118*, 12515.
(29) Chelberg, M. K.; McCarthy, J. B.; Skubitz, A. P. N.; Furcht, L. P.; Tsilybary, E. C. *J. Cell Biol.* **1990**, *111*, 262.
(30) Prime, K. L.; Whitesides, G. M. *Science* **1991**, *252*, 1164.
(31) Sigal, G. B.; Mrksich, M.; Whitesides, G. M. *J. Am. Chem. Soc.* **1998**, *120*, 3464.

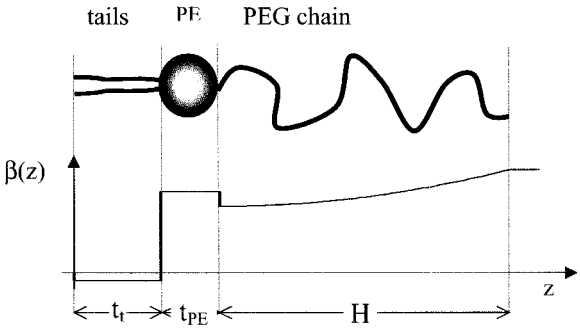

Figure 1. Schematic representation of the box model that was used to fit the reflectivity data of the PEG-lipid monolayers.

The analysis of the experimental data typically started with suggestion of a "box" model that consists of several layers, each having a different scattering length density (β) and thickness (t). To account for surface roughness, the box model was convoluted with a single Gaussian smearing function[11]

$$\beta(z) = \frac{1}{\mathscr{R}(2\pi)^{1/2}} \int_{-\infty}^{\infty} \beta(z') \exp\left[-\frac{(z-z')^2}{2\mathscr{R}^2}\right] dz' \qquad (1)$$

where z is the distance from the interface and $\mathscr{R}$ is the standard deviation of the smearing function. The final form of the scattering length density profile ($\beta(z)$) was divided into a series of 1 Å thick slabs, from which the reflectivity was calculated using the formalism developed by Parratt.[33] Best-fit parameters were determined by minimization of χ^2:

$$\chi^2 = \frac{1}{N_{pts} - N_{par}} \sum_{i=0}^{N_{pts}} \frac{[R_{exp}(q_i) - R_{cal}(q_i)]^2}{\delta_i^2} \qquad (2)$$

where N_{pts} is the number of measured reflectivity values, $R_{exp}(q_i)$ and $R_{cal}(q_i)$ are the reflectivity values calculated from the model, N_{par} is the number of fitted parameters, and δ_i is the measured uncertainty in $R_{exp}(q_i)$.

Results and Discussion

Neutron Reflectivity of PEG-Lipid Monolayers. The box model that was used to fit the reflectivity data of the PEG-lipid monolayers is similar to the one given by Majewski et al.[11] This model consists of three boxes representing the PEG chains, the phosphoethanolamine (PE) layer, and the lipid tails, as illustrated schematically in Figure 1. In an attempt to minimize the number of fitted parameters, we have used for the analysis, whenever possible, previously published data. Choosing each of these values or any combination of them as a fitted parameter had only a minor effect on the results and did not improve the quality of the fit. To gain further insight into the dependence of the structure on the grafting density, the area per molecule was also calculated. The details of the fitting procedure are described later.

The volume fraction of the polymer in the PEG layer (φ_{pol}) was calculated using a relation that was found to describe well other systems of dense polymer brushes[31,34]

$$\varphi_{pol} = \varphi(0)[1 - (z^*/H)^n] \qquad (3)$$

where z^* is the distance from the PE−polymer interface, $\varphi(0)$ is the polymer concentration at $z^* = 0$, H is the brush height, and n is a parameter related to the shape of the volume fraction profile. The scattering length density in this layer was obtained using the relation

$$\beta(z^*) = \varphi_{pol}\beta_{pol} + (1 - \varphi_{pol})\beta_m \qquad (4)$$

where $\beta_{pol} = 0.6 \times 10^{-6}$ Å^{-2} and $\beta_m = 6.38 \times 10^{-6}$ Å^{-2} are the scattering length densities of the PEG and the D_2O subphase, respectively.[13] To account for possible dissolution of molecules in the subphase, the area per molecule (σ^{-1}) was calculated from the reflectivity data by integrating the volume fraction profile, rather than the volume of the spreading solution:

$$\sigma^{-1} = \frac{N v_{EG}}{\int_0^H \varphi(z')\, dz'} \qquad (5)$$

where N is the chain length and $v_{EG} = 61.4$ Å^3 is the volume of an EG monomer.[9]

While three fitted parameters were needed for the PEG layer, the PE layer could be described without any additional parameters. The height of the PE layer was fixed at $t_{PE} = 5.7$ Å.[6] The volume fraction (φ_{PE}) was calculated as $\varphi_{PE} = \sigma^{-1} v_{PE}/t_{PE}$, where $v_{PE} = 243$ Å^3 is the volume of a PE group[6] and the scattering length density in this layer is given by

$$\beta = \varphi_{PE}\beta_{PE} + (1 - \varphi_{PE})\beta_m \qquad (6)$$

where $\beta_{PE} = 2.66 \times 10^{-6}$ Å^{-2} is the scattering length density of PE.[13] The thickness of the tails layer (t_t) was an adjustable parameter. The scattering length density of this layer was calculated from known values for the extended length, the cross section, and the scattering length density (21.7 Å, 42 Å^2, and -0.4×10^{-6} Å^{-2}, respectively[13]) of closely packed lipid tails. The final form of the three-box model was convoluted with a single Gaussian smearing function (eq 1).

The neutron reflectivity curves of the DSPE-PEG5000 and DSPE-PEG2000 monolayers at various grafting densities are shown in Figure 2. The fits to the experimental data, represented as solid lines, were calculated from the best-fit parameters listed in Table 1. The reduced surface densities ($\sigma^* = \sigma\pi R_F^2$), calculated from the Flory radius ($R_F = 3.5N^{0.6}$),[10] are also listed in Table 1. The highest σ^* value for each PEG-lipid corresponds to a monolayer that was compressed to a surface pressure of 40 mN/m, at an area per molecule very close to the monolayer collapse.[26] The volume fraction profiles of the PEG chains, calculated from the best-fit parameters, are shown in Figure 3.

The close agreement between the measured and the calculated reflectivity values strongly suggests that the density profile of the PEG chains can be well-described by a parabolic type equation. This result is analogous to previously studied high molecular weight polymer brushes.[34,35] Furthermore, the high values of n indicate "flattening" of the profile as compared to the parabolic profile ($n = 2$) predicted by the mean field theory.[22] Flattening of the density distribution profile in dense brushes is attributable to configuration constraints introduced to each chain by its neighbor chains.[31] Because of excluded volume effects, displacement of segments from higher (near the interface) to lower concentrations occurs.

(32) Levinski, R. Polymer Brushes and Mesogels in Selectivly Swollen Block Copolymer Films. Ph.D. Thesis, University of Minnesota, Minneapolis, MN, 1996.
(33) Parratt, L. G. *Phys. Rev.* **1954**, *95*, 359.
(34) Kent, M. S.; Lee, L. T.; Factor, B. J.; Rondelez, F.; Smith, G. S. *J. Chem. Phys.* **1995**, *103*, 2320.
(35) Field, J. B.; Toprakcioglu, C.; Ball, R. C.; Stanley, H. B.; Dai, L.; Barford, W.; Penfold, J.; Smith, G.; Hamilton, W. *Macromolecules* **1992**, *25*, 434.

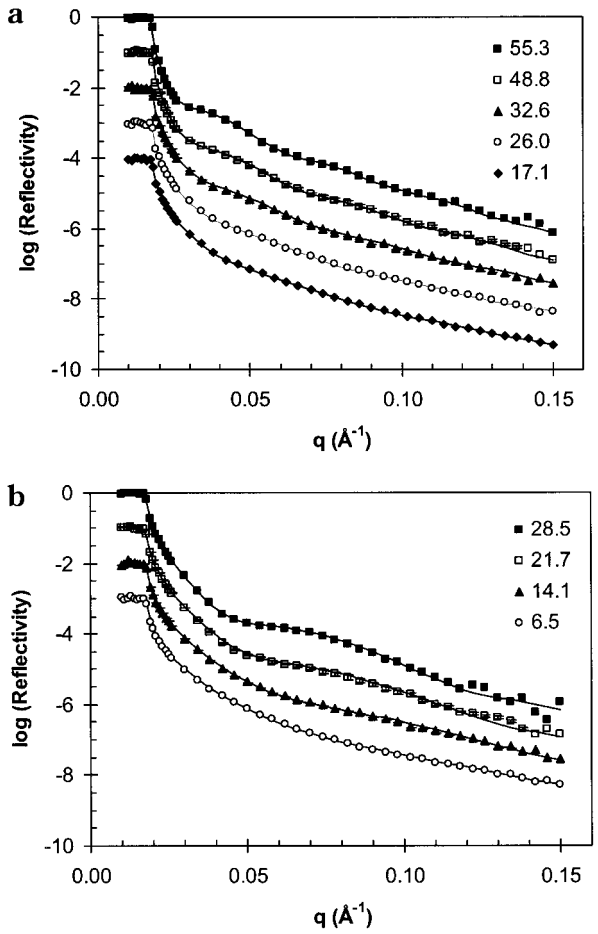

Figure 2. Neutron reflectivity curves of (a) DSPE-PEG5000 and (b) DSPE-PEG2000 monolayers. The legends indicate the reduced surface densities. The solid lines, which represent fits to the experimental data, were calculated from the best-fit parameters listed in Table 1.

Table 1. Best-Fit Parameters for the DSPE-PEG5000 and DSPE-PEG2000 Monolayers

DSPE-PEG5000							
σ^{-1} (Å^2)	σ^*	$\varphi(0)$	H (Å)	n	t_t (Å)	R (Å)	χ^2
202.5	55.3	0.28	174	2.5	18.3	10.4	0.3
229.5	48.8	0.28	159	2.2	18.7	9.3	0.2
342.5	32.6	0.22	145	2.0	17.0	7.5	0.1
431.0	26.0	0.19	129	2.0	18.4	5.8	0.2
654.9	17.1	0.15	110	2.0	17.5	5.8	0.2
DSPE-PEG2000							
σ^{-1} (Å^2)	σ^*	$\varphi(0)$	H (Å)	n	t_t (Å)	R (Å)	χ^2
130.3	28.5	0.31	83	4.9	18.5	11.3	0.3
171.2	21.7	0.26	75	4.0	18.0	9.7	0.4
263.8	14.1	0.23	65	2.5	18.0	7.3	0.2
574.5	6.5	0.19	52	2.0	19.0	5.8	0.1

This becomes more pronounced as the layer is compressed, thus the value of n with increasing surface density (Table 1).

Interestingly, higher values of n were obtained for the DSPE-PEG2000 brushes, even though these monolayers are less crowded than the DSPE-PEG5000 monolayers. This implies that a transition from a parabolic profile to a "flatter" one occurs when the chain length is reduced. The neutron reflectivity curves of the DSPE-PEG750 and the DSPE-PEG120 monolayers, shown in Figure 4, support this suggestion. The fits to the experimental data, represented as solid lines, were calculated from the best-fit parameters listed in Table 2. For these short chains,

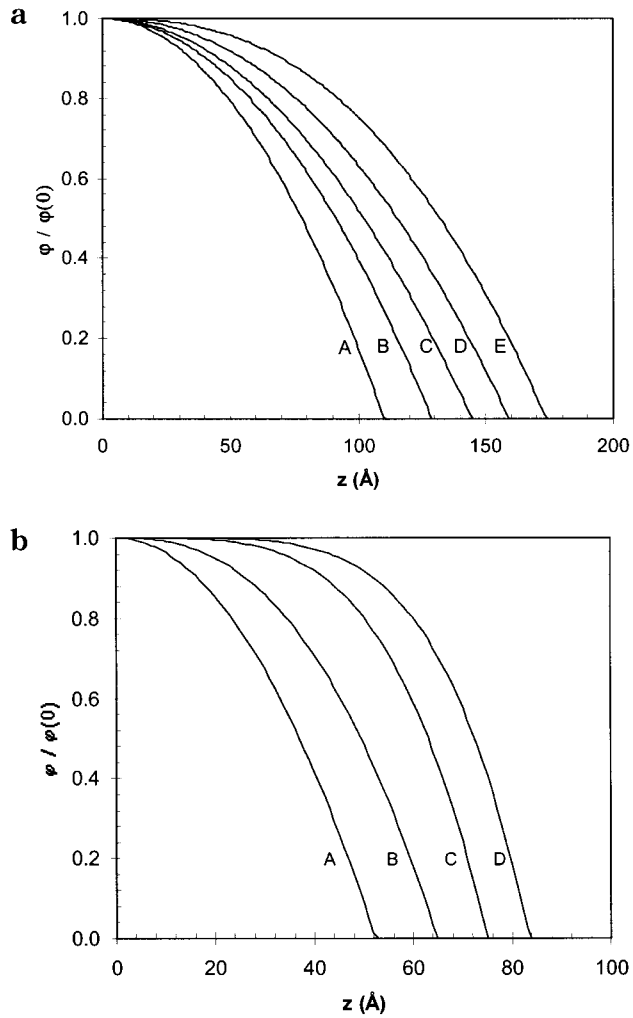

Figure 3. Volume fraction profiles of the PEG segments. (a) DSPE-PEG5000 monolayer, at reduced surface density of (A) 17.1, (B) 26.0, (C) 32.6, (D) 48.8, and (E) 55.3. (b) DSPE-PEG2000 monolayer, at reduced surface density of (A) 6.5, (B) 14.1, (C) 21.7, and (D) 28.5.

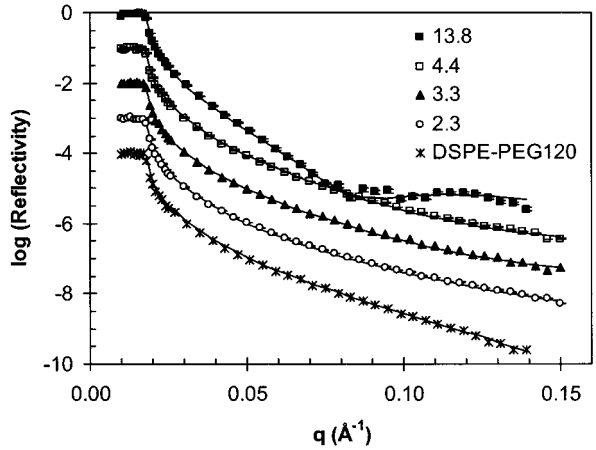

Figure 4. Neutron reflectivity curves of DSPE-PEG750 and DSPE-PEG120 monolayers. The legends indicate the reduced surface densities of the DSPE-PEG750. The solid lines, which represent fits to the experimental data, were calculated from the best-fit parameters listed in Table 2.

replacing the parabolic type profile with a steplike profile (constant polymer concentration, φ_{pol}) was required to obtain a good fit to the experimental data. Thus, while the structure of the PEG5000 brushes agrees with the mean field description, the segmental distribution of the

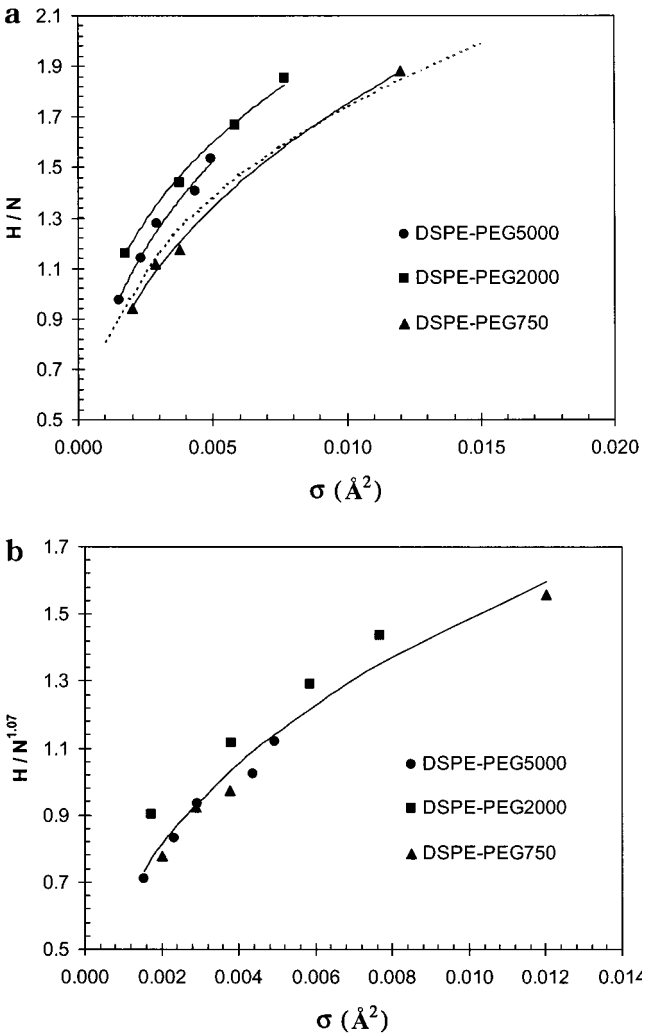

Figure 5. (a) Dependence of the brush height, H, normalized to the chain length, N, on the surface density. The solid lines represent best fits to power law relations. (b) A comparison between the experimental brush height and the best-fit power law relation, $H \sim N^{1.07}\sigma^{0.38}$.

Table 2. Best-Fit Parameters for the DSPE-PEG750 and DSPE-PEG120 Monolayers

DSPE-PEG750						
σ^{-1} (Å^2)	σ^*	φ_{pol}	H (Å)	t_t (Å)	R (Å)	χ^2
83	13.4	0.42	32	18.3	7.8	0.5
265	4.4	0.21	20	18.7	5.0	0.3
345	3.3	0.17	19	18.0	4.0	0.3
497	2.3	0.14	16	17.5	3.5	0.2
DSPE-PEG120						
σ^{-1} (Å^2)	σ^*	φ_{pol}	H (Å)	t_t (Å)	R (Å)	χ^2
45		0.55	10	20.0	7.5	0.6

PEG750 chains seems to follow the scaling approach.[15] In this sense, the PEG2000 brushes can be considered to be an intermediate case between these theories.

A comparison of the brush height with the theoretical predictions is shown in Figure 5a. The solid lines in Figure 5a represent best fits to power law relations, with exponents of 0.37, 0.31, and 0.38 for DSPE-PEG5000, DSPE-PEG2000, and DSPE-PEG750, respectively. These values are in fairly good agreement with the third power law dependence predicted by both theories. In particular, the height of the DSPE-PEG750 brushes is well-described by the prediction of the scaling theory, shown as a dashed line in Figure 5a. To determine the dependence of the brush height on the chain length, we fit the entire range of data to a power law. A best fit was obtained using $H \sim N^{1.07}\sigma^{0.38}$, as shown in Figure 5b.

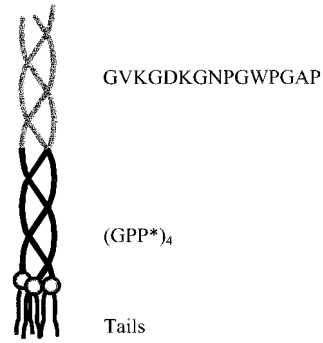

Figure 6. Schematic illustration of the $(C_{16})_2$-Glu-C_2-$(GPP^*)_4$-IVH1 peptide-amphiphile.

Neutron Reflectivity of the Peptide-Amphiphile Monolayers. The schematic structure of the peptide-amphiphile used in this study is shown in Figure 6. The hydrophilic headgroup is a 27 amino acids sequence, attached to a flexible spacer.[27] We have previously shown[28] that the peptide is folded into a triple-helical conformation. Although such a conformation is expected to hinder most of the motions with respect to the peptide backbone, the presence of the spacer may allow tilting of the head. The extended length of the peptide-amphiphile headgroup was approximated to be 87 Å from known amino acid sizes[36] and bond lengths.

The neutron reflectivity curves for layers of the $(C_{16})_2$-Glu-C_2-$(GPP^*)_4$-IVH1 peptide-amphiphile at various surface pressures, on a pure D_2O subphase and on a 50% D_2O subphase, are shown in Figure 7. The fits to the experimental data, represented as solid lines, were obtained using a simple two-layer box model with a Gaussian smearing (eq 1); one layer represents the hydrocarbon tails, and the other layer represents the peptide headgroup. The values of the fitted parameters are listed in Table 3.

The consistency of the simplified box model requires that the scattering length density of the tail layer (β_t) and the height of both layers be identical for both contrasts. The scattering length density of the head layer (β_h) was calculated using $\beta = \varphi\beta_p + (1 - \varphi)\beta_m$, where $\beta_p = 2.6 \times 10^{-6}$ Å^{-2}, the scattering length density of the peptide headgroup, was estimated from its chemical structure. The volume fraction of the peptide (φ) was used as a fitted parameter. The best fits for all monolayers were obtained with a value of $t_t = 20$ Å for the tails layer. As a test for the accuracy of the fitting, the volume of the peptide headgroup (v) was calculated using

$$v = At_h\varphi \tag{7}$$

The area per molecule (A) was approximated from the surface pressure−area isotherm.[26] This value was found to be constant (within ±10%) for all four monolayers. It should be noted that several other models, accounting for variations of the scattering length along the peptide, could fit the experimental data. However, none of these models gave a better statistical fit than the simplified two-layer model, and they all gave the same overall height for the peptide layer.

(36) Creighton, T. E. *Proteins*: *Structure and Molecular Proteins*; W. H. Freeman and Company: New York, 1993.

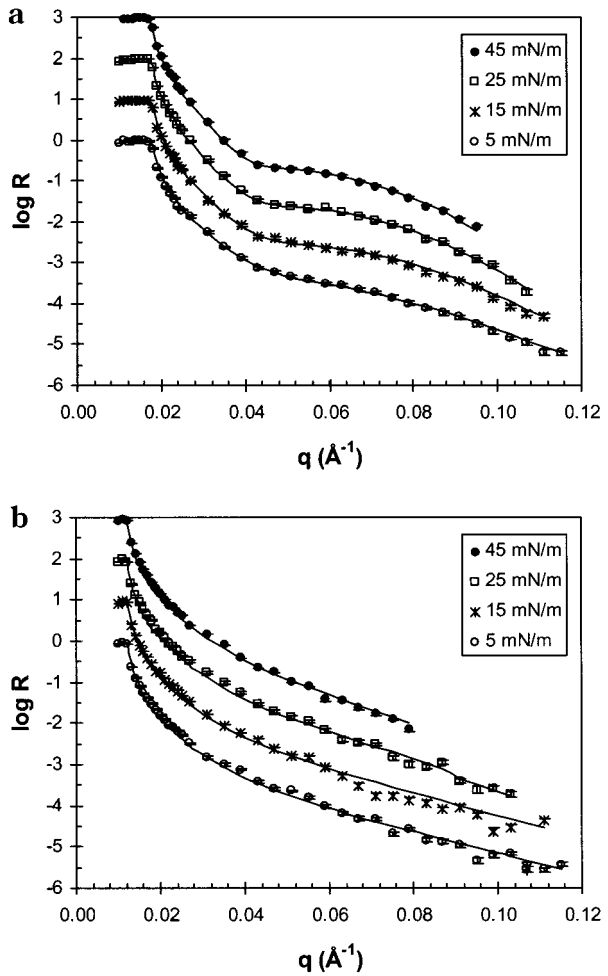

Figure 7. Neutron reflectivity curves of the $(C_{16})_2$-Glu-C_2-$(GPP^*)_4$-IVH1 peptide-amphiphile (a) on a pure D_2O subphase and (b) on a 50% D_2O subphase. The legends indicate surface pressure. The solid lines, which represent fits to the experimental data, were calculated from the best-fit parameters listed in Table 3.

Table 3. Best-Fit Parameters for the Peptide-Amphiphile Monolayers

π (mN/m)	φ_p	H (Å)	R (Å)	χ^2
40	0.47	86	16.0	0.6
25	0.46	84	13.3	0.8
15	0.40	81	10.5	1.2
5	0.30	80	9.5	1.6

At the highest surface pressure, the thickness of the headgroup layer is very close to its calculated extended length, indicating that the peptide is oriented perpendicular to the air−water interface. Moreover, a decrease in the surface pressure results in only a small decrease in the layer height, indicating that the upright orientation is nearly not affected. At the lowest surface pressure, the layer height corresponds to tilting at an angle of about 20° with respect to the normal to the interface.

Neutron Reflectivity of Mixed Peptide-Amphiphile/PEG-Lipid Monolayers. The general box model that was used to describe the structure of a monolayer composed of a mixture of a PEG-lipid and a peptide-amphiphile is described schematically in Figure 8. This model consists of four boxes: (i) the tail region, (ii) a layer containing the peptide-amphiphile headgroups and the PEG-lipid PE groups, (iii) a layer that contains the peptide-amphiphile headgroups and the PEG chains, and (iv) a layer containing either the peptide-amphiphile headgroups or the PEG chains, depending on the length of the PEG chains.

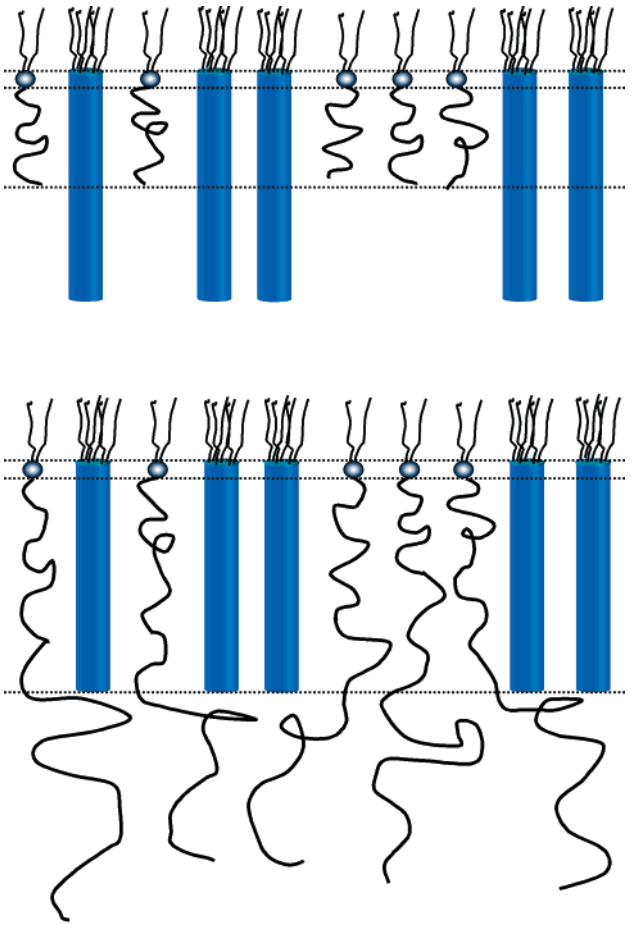

Figure 8. Schematic representation of the box model that was used to fit the reflectivity data of the monolayers composed of a mixture of a PEG-lipid and a peptide-amphiphile.

The simplest situation that one can consider is that each of the membrane components will retain the same structure as in the single-component monolayer. Practically, this means that the volume fraction of the peptide-amphiphile headgroup does not change along the *z*-axis, and the PEG volume fraction profile is parabolic or steplike, depending on the chain length. We have applied this approach to the analysis of neutron reflectivity curves measured from mixed monolayers compressed to a surface pressure of 40 mN/m. The height of the tail region, the parameters describing the brush structure, and the peptide volume fraction were used as fitted parameters. The length of the peptide-amphiphile headgroup was assumed to be 86 Å. The scattering length density in each layer was determined when the scattering length densities of its components were averaged.

When this simplified approach is used, a good fit is obtained to the reflectivity of mixtures with DSPE-PEG2000 (Figure 9) and DSPE-PEG750 (data not shown). For both of these mixtures, the height of the brush did not change as compared to a "pure" PEG-lipid monolayer at the same surface pressure. However, the value of n for the PEG2000 brush increased considerably, from $n = 4.9$ in the pure monolayer to $n = 7.8$ in the mixed monolayer, indicating additional flattening of the profile. This effect can be attributed to enhanced configurational constraints, imposed by the stiff peptide-amphiphile headgroup in the layer.

The enhanced configurational constraint that the peptide-amphiphile imposes on the PEG chains leads to an

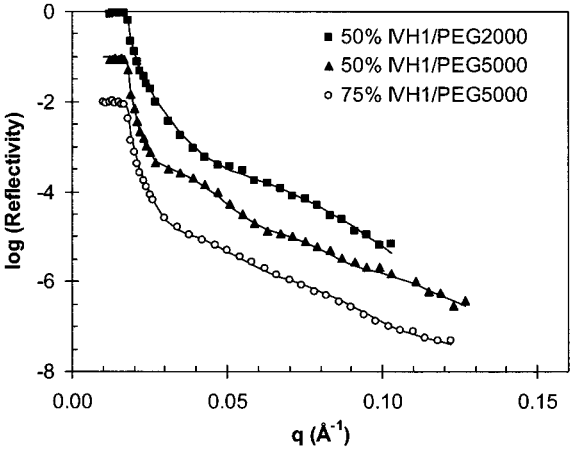

Figure 9. Neutron reflectivity curves of monolayers composed of a mixture of a PEG-lipid and a peptide-amphiphile. The solid lines represent best fits to the experimental data.

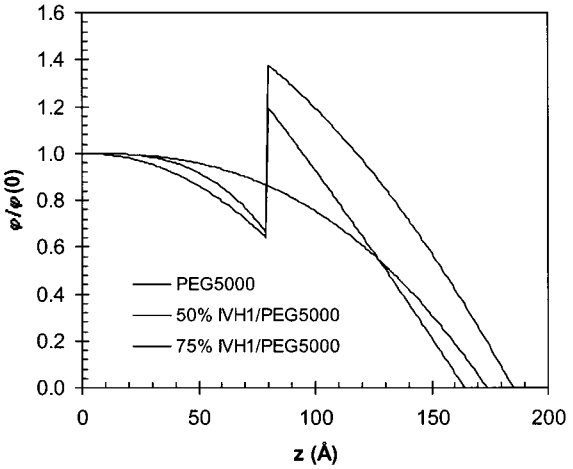

Figure 10. Comparison between the volume fraction profiles of the PEG segments in a single-component DSPE-PEG5000 monolayer and in monolayers composed of a mixture with a peptide-amphiphile.

unusual concentration profile in the DSPE-PEG5000 mixed monolayer. For these curves, a good fit to the experimental data could not be obtained under the assumption that the brush retains its unperturbed structure. However, a good fit was obtained using an analogy between the PEG5000 brush in this mixed monolayer and the long brush in a bidispersed mixture of short and long chains.[31] In both cases, the excluded volume effects are reduced considerably at some distance from the wall, for which only segments of the long chain are present. The fits shown in Figure 9 were obtained using a superposition of two parabolic type profiles as suggested for a bidispersed system. The resulting volume fraction profiles are compared in Figure 10 to the profile in a single-component DSPE-PEG5000 monolayer. The sudden increase in the polymer concentration at the edge of the peptide-amphiphile head is very pronounced. In studies of bidisperse polymer brushes,[31,37] the longer chain was found to have a maximum concentration at z values corresponding to the total length of the shorter chain. It should be noted, however, that in bidisperse systems the two types of chains are free to rearrange themselves. Moreover, the constantly decreasing concentration of the shorter chain along the z-axis leads to a gradual decrease in the configurational constraints. In contrast, the constraint introduced by the peptide is constant. When this constraint is removed at once, a sudden increase in the area available for each chain results in a more "relaxed" configuration.

Conclusions

We have studied the structure of Langmuir monolayers containing a PEG-lipid, a peptide-amphiphile, or a binary mixture of both using neutron reflection. The experimental data were best fitted using a parabolic type equation or a step function to describe the PEG segmental concentration profiles, depending on the chain length. The profiles obtained for DSPE-PEG5000 and DSPE-PEG2000 monolayers were parabolic at low grafting densities and became flatter when the area per molecule was reduced. On the other hand, a better fit was obtained with a steplike profile for the DSPE-PEG120 and the DSPE-PEG750 monolayers. The brush height was in close agreement with the predictions of the self-consistent mean field and the scaling theories and was best fitted to the power law $H \sim N^{1.07}\sigma^{0.38}$. In monolayers that contained the peptide-amphiphile as a single component, the headgroup was found to be oriented perpendicular to the air−water interface. Incorporation of the peptide-amphiphile into a PEG-lipid monolayer enhanced the configurational constraints and resulted in perturbation of the brush structure. Additional flattening of the profiles was observed in the DSPE-PEG2000 brush, which has a similar thickness to the peptide-amphiphile headgroup. A sudden increase in the polymer concentration at the edge of the peptide-amphiphile head, which was attributed to relaxation of the chains, was observed in the DSPE-PEG5000 brushes that are much longer than the peptide. We are using this surface conformation information to design biologically functional surfaces with controlled accessibility of ligands.

Acknowledgment. The authors acknowledge with gratitude support from the US−Israel Binational Science Foundation (1999225), the National Institutes of Health (HL62427-01), and the MRSEC Program of the National Science Foundation (DMR-0080034).

LA990383I

(37) Kent, M. S.; Factor, J. B.; Satija, S.; Gallagher, P.; Smith, G. S. *Macromolecules* **1996**, *29*, 2843.